Self-association of long-acting insulin analogues studied by size exclusion chromatography coupled to multi-angle light scattering

Malene H. Jensen [a,b,c,*], Per-Olof Wahlund [c], Jes K. Jacobsen [c],
Bente Vestergaard [a,b], Marco van de Weert [b], Svend Havelund [c,**]

[a] Department of Medicinal Chemistry, Faculty of Pharmaceutical Sciences, University of Copenhagen, Universitetsparken 2, DK-2100 Copenhagen-Ø, Denmark
[b] Department of Pharmaceutics and Analytical Chemistry, Faculty of Pharmaceutical Sciences, University of Copenhagen, Universitetsparken 2, DK-2100 Copenhagen-Ø, Denmark
[c] Novo Nordisk A/S, Novo Nordisk Park 1, DK-2760 Måløv, Denmark

ABSTRACT

Two structurally very different insulin analogues analysed here, belong to a class of analogues of which two have been reported to have a protracted action through self-assembly to high molar mass in subcutis. The process of self-association of insulin analogues Lys^{B29} (N$^\varepsilon\omega$-carboxyheptadecanoyl) des(B30) human insulin and Lys^{B29} (N$^\varepsilon$-lithocholyl) des(B30) human insulin was investigated using size exclusion chromatography (SEC) in connection with multi-angle light-scattering. Self-assembly to high molar mass was obtained by exchanging the formulation containing phenolic preservatives with an isotonic eluent during SEC. It was shown that increasing amounts of zinc in the formulations of the two analogues increased the size of the self assemblies formed during gel filtration. The addition of 0.2 mM phenol to the elution buffer slowed down the self-association process of zinc containing formulations and shed light on the initial association process. The results indicated that a dihexamer is a possible building block during self-association of Lys^{B29} (N$^\varepsilon\omega$-carboxyheptadecanoyl) des(B30) human insulin. Surprisingly, in the absence of zinc the two analogues behaved very differently. Lys^{B29} (N$^\varepsilon\omega$-carboxyheptadecanoyl) des(B30) human insulin was in equilibrium between oligomers smaller than a hexamer, whereas Lys^{B29} (N$^\varepsilon$-lithocholyl) des(B30) human insulin self-associated and formed even larger complexes than in the presence of zinc.

© 2011 Elsevier B.V. All rights reserved.

1. Introduction

During the last couple of decades, there has been an intense interest in developing new insulin pharmaceutics beneficial to diabetics. Diabetes is a disease with an expected epidemic increase in the next couple of decades, especially in the developing world [1], which can have severe negative impacts for the patients. For this reason it is of key importance to develop new and improved insulin molecules, which can ensure the patients a secure, effective, and comfortable treatment.

The active insulin molecule in human is a short two-chained protein of 21 and 30 amino acids (A- and B-chains, respectively) with a molar mass (MM) of 5.8 kDa. Insulin has a natural tendency to self-associate into dimers and hexamers, in particular in the presence of Zn(II) ions [2–4].

Different strategies have been used to develop new insulin molecules with specific functions. Fast-acting insulin has been developed to resemble the spikes in insulin levels of a healthy person in connection with meals [5–7], while the long-acting insulin analogues are designed to mimic the basal level of insulin through the whole day [8–11].

A more recent strategy is to attach human serum albumin (HSA) binding side chains, e.g. through acylation. These acylated insulin analogues were designed to obtain their protracted activity by reversible binding to HSA in the subcutaneous (s.c.) depot and in the blood stream [12–15]. However, later studies showed that albumin-binding was not the only reason for protraction and that self-association consolidates the effect. An example of this type of analogues is the clinically available insulin detemir, LysB29 (N-tetradecanoyl) des(B30) human insulin [16–18]. Other acylated insulin analogues were shown to self-assemble into very large high MM complexes while remaining in solution, and have even longer action than facilitated by HSA binding and the
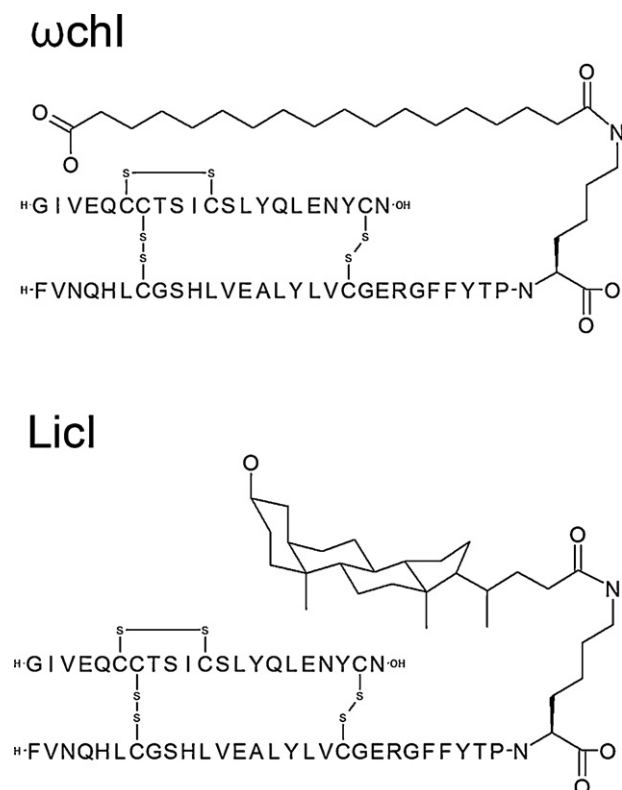
Fig. 1. Chemical structures of human insulin analogues Lys^{B29} (N$^\varepsilon$ω-carboxyheptadecanoyl) des(B30) human insulin (ωchI) and Lys^{B29} (N$^\varepsilon$–lithocholyl) des(B30) human insulin (licI). The two structures show the chemical modification of the two analogues, where a carboxy-fatty acid- or a lithocholyl-side chain, respectively, is attached at lysine B29 to human insulin lacking threonine B30.

comparatively smaller oligomers observed for insulin detemir [13,18,19]. Such high MM assemblies form a small s.c. depot, which slowly releases insulin into the blood. In the blood, binding to HSA further prolongs the action also of this class of analogues. An example of a self-associating analogue forming high MM assemblies is insulin Degludec (IDeg) [20–23], which has recently passed phase II trials.

The two analogues under scrutiny in this study represent two types of acylated insulin analogues namely fatty di-acid acylated insulin analogues with a terminal carboxy group [24,25] and lithocholyl acylated analogues [25,26], Lys^{B29} (N$^\varepsilon$ω-carboxyheptadecanoyl) des(B30) human insulin (ωchI) and Lys^{B29} (N$^\varepsilon$-lithocholyl) des(B30) human insulin (licI), respectively (see Fig. 1). This type of protracted insulin analogues is stabilised by the addition of zinc ions and phenol and hence are anticipated to be in the 'relaxed' (R$_6$) hexameric state in the formulation.

In the formulation used for s.c. injection, the analogues are anticipated to form hexamers in the 'relaxed' state (R$_6$) because of the presence of Zn(II) and phenol, analogous to unmodified insulin. The two Zn(II) ions bind in the central axis of the insulin hexamer, and phenol binds in small pockets in the dimer interfaces of the hexamer, forming R$_6$-stabilising interactions [27,28]. The presence of phenol or phenolic derivatives controls in this way the conformational state adopted by the hexamer. Consequently, when phenol disappears from the injection site, as a result of diffusion, a conformational change transforms the hexamer to the 'tense' state (T$_6$). Large-scale association and formation of large high MM associates requires the (modified) insulin to be in this T$_6$ state [19,26]. The R and T state differ in the secondary structure of the N-terminal part of the B-chain in the insulin monomer, where the first eight amino acids form an α-helix or an extended conformation,

respectively. The R$_6$, intermediate T$_3$R$_3$, and T$_6$ states were first discovered in crystal structures [27,29,30] and have since been studied thoroughly in solution [31,32].

The two analogues have previously been investigated by different size exclusion chromatography (SEC) systems in isotonic elution conditions. ωchI has been reported to form large aggregates eluting in the void volume in the presence of 2 and 3 Zn(II) per six insulin monomers (/6 Ins) on a Sephacryl S-300 HR column using a phosphate buffered isotonic eluent similar to the system presented here. Aggregates are not formed in the absence of zinc. licI was analysed in another complementary SEC system using a Superose 6 HR column and a Tris–HCl buffered isotonic eluent. In the presence of 2 and 3 Zn(II)/6 Ins, licI elutes in or close to the void volume. The SEC results were compared to albumin binding assays and disappearance half-times in pigs, showing that ωchI and licI display the same analytical profile as IDeg and Lys^{B29} (N$^\varepsilon$-lithocholyl-γ-Glu) desB30 human insulin (ligI), respectively, that both display protracted profiles in clamp studies in pigs [19,21]. With the addition of phenol to a high concentration in the eluent, no high MM associates are formed of the lithocholyl acylated analogue which elutes with an apparent size of an insulin monomer [19,26] – indicating that no self-association happens in the presence of phenol and zinc, where unmodified human insulin is known to be in the R$_6$ hexameric state. The insulin analogue ligI shows largely the same behavior as licI, although in the presence of phenol in the eluent it elutes as a dihexamer [19]. A SEC study of insulin detemir shows that this analogue does not self-associate above a dihexamer, and owes its protracted effect to dihexamer formation as well as HSA binding [18].

Here, an extensive analysis of the self-association properties of two protracted insulin analogues is presented. We investigate the effect of the relative zinc concentration, the presence of phenol in the SEC eluent, and the sample concentration. Chromatographic analysis is coupled with multi-angle light scattering (MALS) measurements, yielding invaluable information not available without MALS, thereby providing results contributing significantly to the already accumulated knowledge and in some cases changing the current understanding of the self-associated states of the analogues. The combination of these two techniques significantly increases our understanding of the self-association processes that are likely to take place upon injection of the zinc- and phenol-containing formulations of these protracted insulin analogues. This insight may be used to further improve these insulin analogues and their formulation.

2. Materials and methods

2.1. Preparation and formulation of insulin analogues

The two acylated insulin analogues, ωchI and licI, were synthesised and purified as previously described [24,33]. The sample composition was 1200 μM insulin analogue, with 0, 3, or 6 Zn^{2+} ions per hexamer, 10 mM Tris–HCl pH 7.4, and 32 mM phenol, which is similar to the standard composition for clinical use. In the following, the samples will be named according to the insulin analogue (ωchI or licI) and the number of Zn^{2+} ions per six insulin molecules (e.g. ωchI_3Zn). Phenol is used both as a preservative in the formulation, and to keep the insulin hexamers in the R state.

All chemicals were analytical grade reagents.

2.2. Size-exclusion chromatography

Size-exclusion chromatography (SEC) was used as a method for characterisation of the self-association of the insulin analogues. The SEC system is designed to mimic the events during s.c. injection where the preservatives and components from the formulation are

replaced by the interstitial fluid. Therefore, the elution buffer consists of an isotonic saline solution as described by Havelund et al. [18].

SEC was carried out on an Agilent 1200 Series HPLC (Agilent Technologies). A Superdex 200 GL 10/30 column with a separation range of 10–600 kDa (GE Healthcare) and an eluent containing 10 mM Tris–HCl, pH 7.4, 140 mM NaCl, and 0.01% NaN$_3$ were used for separation at room temperature. All chemicals were analytical grade reagents, and buffers were made with Milli-Q grade water (Millipore) and filtered through a 0.2 μm filter prior to chromatographic analysis. For analysis of ωchI a small amount of phenol (0.2 mM) was added to the elution buffer in order to slow down the process and facilitate separation of different states in the self-association process of ωchI. A sample volume of 200 μL was injected onto the column and the separation was performed with a flow of 0.5 mL/min. The chromatograms are represented with the available volume of the column, K_D:

$$K_D = \frac{V_e - V_0}{V_t - V_0}$$

where V_e is the elution volume of a peak, V_0 is the void volume, and V_t is the total volume. The retention time of Blue Dextran and insulin mutant B9Asp/B27Glu (monomeric insulin) [5,34] was used as V_0 and V_t, respectively.

As MM standards blue dextran (≥2000 kDa), thyroglobulin (669 kDa), ferritin (440 kDa), human serum albumin (HSA, 67 kDa), ovalbumin (43 kDa) and ribonuclease (12.6 kDa) were used. Furthermore, Cobalt (III) Insulin (Co(III), hexameric insulin, 35 kDa) [35] and insulin mutant B9Asp/B27Glu (∼6 kDa) [5,34] were used as insulin standards. The number averaged MM (M_N) derived from SEC was obtained from a standard curve of the above mentioned standards with the exception of Blue Dextran and insulin mutant B9Asp/B27Glu, because they are outside the separation range of the column.

2.3. Multi-angle light scattering

MALS is a technique for the determination of the absolute molar mass and size of macromolecules in solution. Details on MALS measurements and calculations in connection with SEC are described in Wen et al. [36]. MALS was performed in connection with SEC runs of the two analogues in order to obtain a weight average MM (M_W) of the species being separated as well as the radius of gyration (R_g) and the hydrodynamic radius (R_H) when possible. Every sample was run at least twice to ensure consistency between different SEC/MALS runs at the same conditions. Because of the presence of equilibria between different oligomeric species in the samples, reproducibility with standard deviations for the absolute M_W was not performed. Instead, one chromatogram of each sample was chosen to represent the system.

A static light scattering instrument with 18 photo detectors (DAWN® HELEOS™) was connected to the HPLC, along with a differential refractometer (Optilab® rEX™), and one detector is replaced by a dynamic light scattering (DLS) detector (WyattQELS™). All instruments are from Wyatt Technology Inc. The signal from UV$_{276}$, refractive index (RI), DLS, and MALS was collected continuously.

Calculation of M_W was performed with the software ASTRA® V also from Wyatt Technology Inc using the measured MALS- and UV$_{276}$-signal, and a refractive index increment (dn/dc) of 0.185 mL/g (a typical value for proteins) [36] and the Zimm's equation:

$$K^* \frac{c}{R_\theta} = \frac{1}{M_W P_\theta} + 2A_2 \tag{1}$$

where c is the concentration of the solute (g/mL), M_W is the weight averaged molecular mass, R_θ is the Rayleigh ratio, A_2 is the second virial coefficient, P_θ is the scattering function. The optical constant, K^*, can be calculated as:

$$K^* = 4\pi^2 n_0^2 \left(\frac{dn}{dc}\right)^2 N_A^{-1} \lambda_0^{-4} \tag{2}$$

where n_0 is the refractive index of the solvent, dn/dc is the refractive index increment, N_A is Avogadro's number, and λ_0 is the wavelength of the light in vacuum. The M_W was only determined in the chromatographic regions where both the UV$_{276\,nm}$ (or RI) and MALS signal was sufficiently high. Extinction coefficients of 1037.84 and 1070.64 g/mL/cm were used for ωchI and licI, respectively, to calculate the concentration of the analogues throughout the chromatographic run. The recovery of the sample was calculated from the injected and recovered mass. The recovery of the samples was always above 90%, except for licI_0Zn, where the recovery was 75%.

Finally, the radius of gyration, R_g, also known as the root mean square radius, was calculated through the scattering function, P_θ:

$$P_\theta = 1 - \frac{q^2 R_g^2}{3} \tag{3}$$

where q is the scattering vector.

2.4. Dynamic light scattering

DLS was used to determine the R_H of the sample both online and in batch measurements. For a more detailed review of DLS theory see Pecora [37]. In connection with SEC the online DLS signal was used to determine the R_H of the sample by the Stokes–Einstein equation which relates to spherical particles:

$$R_H = \frac{k_B T}{6\pi \eta D_\tau} \tag{4}$$

where k_B is the Boltzmann constant, T is the temperature, η is the solvent viscosity, and D_τ is the translational diffusion coefficient. D_τ can be calculated from the decay rate ($\Gamma = D_\tau q^2$). Γ is calculated from the autocorrelation function which is a measure of the intensity fluctuations of the particle in solution:

$$G(\tau) = A + Be^{-2\Gamma \tau} \tag{5}$$

A and B are instrumental factors, and τ is the time delay. It was not possible to calculate the R_H for all the samples, as those with $M_W > 1000$ kDa did not give a measurable DLS signal.

For batch measurements of the samples prior to SEC, DLS was measured on a DynaPro™ Platereader from Wyatt Technology Inc. employing the same theory as for online measurements. The samples were measured in the formulation conditions as described above with 30 aquisitions of 10 or 30 s and were analysed using the DYNAMICS® software.

2.5. Shape prediction from M_W, R_g, and R_H

Information about the shape of a particle in solution can be obtained from a combination of the parameters M_W, R_g, and R_H.

The R_g/R_H ratio (ρ) gives an indication of the shape of the molecule, where ρ is 0.78 for a spherical molecule and >2 for a rod-shaped molecule [38]. In effect, it provides an estimation of the deviation of the shape from a homogenous spherical particle. In the case of a rod, the ρ value depends on the length and radius of the rod. Another shape prediction can be obtained from the log(R_g) versus log(M_W) conformation plot. A slope of 0.33, 0.5, or 1 is descriptive of a sphere, coil, or rod [39], respectively.

Table 1
Summary of the SEC and MALS results obtained for Lys[B29] (N$^{\varepsilon}$ω-carboxyheptadecanoyl) des(B30) human insulin and Lys[B29] (N$^{\varepsilon}$-lithocholyl) des(B30) human insulin formulated with 0, 3, and 6 Zn(II)/6 Ins. The M_W of the peaks and the M_W distribution covering the peak range in Fig. 2 are shown.

Sample	Peak M_W (kDa)	Peak-range M_W distribution (kDa)
licI_0Zn	21,200	8700–132,000
licI_3Zn	130	72–370
licI_6Zn	480; 2600	130–2300
ωchI_0Zn	21	9–20
ωchI_3Zn	12; 3800	11–15; 3300–4300
ωchI_6Zn	70[b]; 4100	68–75; 3000–4600
ωchI_0Zn_ph[a]	22	8–23
ωchI_3Zn_ph[a]	82[c]; 190; 280	82–570
ωchI_6Zn_ph[a]	47[b]; 95[c]; 180; 360	30–590

[a] Eluent containing 0.2 mM phenol.
[b] The peak discussed in the text with a $K_D = 0.72$ in Fig. 2b and c.
[c] The peak discussed in the text with a $K_D = 0.65$ in Fig. 2c.

3. Results and discussion

The self-association of two structurally different acylated analogues that are investigated here is induced *in vivo* by diffusion of phenol away from the site of injection. Here, we use SEC-based buffer exchange to mimic the process.

Varying the amount of zinc ions in the formulation affected the degree of self-association of the two analogues. The self-association dependency on zinc ions was therefore analysed with SEC–MALS for both insulin analogues. After preliminary tests, the conditions with 0, 3, and 6 Zn(II)/6 Ins were chosen for further experiments. The results are summarized in Table 1 and Fig. 2.

The R_H was used to estimate the oligomerisation state of the samples prior to higher self-assembly on the SEC column. The dimensions of human insulin in the hexameric R_6-state (from crystal structure: PDB ID 1EV3) with an oblate spheroid shape are ~5 nm in diameter and ~4 nm in height [40]. The R_H of hexameric insulin has previously been reported to be 2.8 nm [4]. Finally, calculation of R_H from human insulin R_6-hexamer and R_6-dihexamer using the program HYDROPRO [41] resulted in 2.6 and 3.4 nm, respectively. DLS measurements of the samples, ωchI_0Zn, ωchI_3Zn, and ωchI_6Zn, resulted in R_Hs of 1.6, 2.6, and 2.6 nm, respectively, thus suggesting samples of hexameric size in the presence of zinc and a smaller oligomeric state in the absence of zinc. DLS measurements of licI_0Zn revealed an R_H of 2 nm, licI_3Zn with a R_H of 3.6 nm, and licI_6Zn revealed a bimodal sample with two species of 2.7 (84 mass%) and 6.2 nm (16 mass%). Thus in the presence of zinc, licI is larger than ωchI whereas in the absence of zinc it is also expected to be smaller than a hexamer.

3.1. Self-association of Lys[B29] (N$^{\varepsilon}$-lithocholyl) des(B30) human insulin

The chromatography of licI in formulations with 0, 3, and 6 Zn(II)/6 Ins revealed that this analogue formed high-MM associates in different size ranges depending on the amount of zinc present in the formulation (see Fig. 2a). licI_0Zn eluted in the low-MM range of the column, licI_3Zn in the middle of the column volume (CV), and licI_6Zn in the void volume.

In Fig. 2a, the MALS determined M_W can be seen together with the corresponding chromatograms. The two samples, licI_3Zn and licI_6Zn, gave rise to peaks with M_W in the ranges 72–370 and 130–2300 kDa. This was comparable with the M_N-range expected from standard SEC calibration, but M_W gave a better measure of the mass of licI_6Zn, as it elutes in the void volume of our SEC column. For our system this means that masses above 600 kDa cannot be estimated by a SEC standard curve.

When examining the chromatogram of licI_0Zn (Fig. 2a), the protein elutes in the low-MM range of the column corresponding to a low M_N; however, M_W reveals significantly larger assemblies with a mass difference of about three orders of magnitude (8700–132,000 kDa, see Table 1). The apparent associated state of licI in the absence of zinc ions as determined by MALS did not correspond with the elution of the sample in the low-MM range of the column. Thus, these results strongly suggest that self-association of licI also happens when zinc is not present. Since divalent cations are needed for hexamer formation, it is very likely, that zinc-free licI self-association was formed from the monomeric and dimeric states of insulin. In these quaternary states, the hydrophobic surface areas of the insulin molecule, otherwise hidden in the hexamer, were exposed and interaction with the highly hydrophobic cholic side chains was possible. It is therefore likely that this type of self-association is of an entirely different nature than when zinc is present. It is presumed that self-association happens on the column when phenol is removed and the ion strength is increased, however, the self-association may continue after the column. Another reason for the elution profile with high M_W in the low-MM range could be that licI_0Zn travels through the column as a low MM species, smaller than an insulin hexamer (as indicated by the pre-self-association R_H), thus self-association happens in the time between the sample leaves the column and before it reaches the MALS detector. Both reasons are possible and they may combined be responsible for the high M_W. Furthermore, it could be seen that a part of this sample eluted after the separation range of the column, which indicated that other effects than ordinary gel filtration was responsible for the elution profile. This was supported by the relatively low recovery of the sample within the exclusion range of the column (74%); however, when including also the tailing slope of the peak outside the separation volume the recovery was 96%. In fact, a part of the high-MM sample licI_0Zn, eluted later than the insulin monomer standard from the SEC column. We suggest the possible explanations: Either, the sample forms hydrophobic interactions with the column material. Or, upon removal of phenol self-association may have induced an increased viscosity of the sample on the column due to salting out effects. Both scenarios may be jointly responsible for disturbing a standard elution of the sample.

Apart from the zinc dependence, the effect of initial protein concentration on the degree of self-association was also investigated. In order to do so, different licI concentrations (150, 600, and 1200 μM) were tested for all three zinc formulations (data not shown). In the presence of zinc, the self-association of licI was dependent on the mass of protein loaded on the column; the self-assembly of licI moved towards higher MM on the SEC column with higher start concentrations. For licI_0Zn, however, the injected mass did not have a significant influence, and the peak eluted as described above.

3.2. Self-association of Lys[B29] (N$^{\varepsilon}$ω-carboxyheptadecanoyl) des(B30) human insulin

Insulin analogue ωchI was analysed in the same manner. In the absence of zinc, ωchI eluted in a peak with a M_W of 9–20 kDa, i.e. covering oligomers smaller than a hexamer and is equal to the mass obtained from the insulin standards (see Fig. 2b). The slope of the MALS M_W determination for this peak indicates that the peak consisted of several oligomers in equilibrium in the absence of zinc ions. These oligomers may be monomers, dimers, trimers, and tetramers of ωchI, but exactly which oligomers are not revealed by these data.

In the presence of both 3 and 6 zinc ions (Fig. 2b) ωchI eluted in the void volume with extensive tailing indicating that the peak consists of a distribution of sizes. The determination of M_W of the two formulations ωchI_3Zn and ωchI_6Zn showed a high MM self
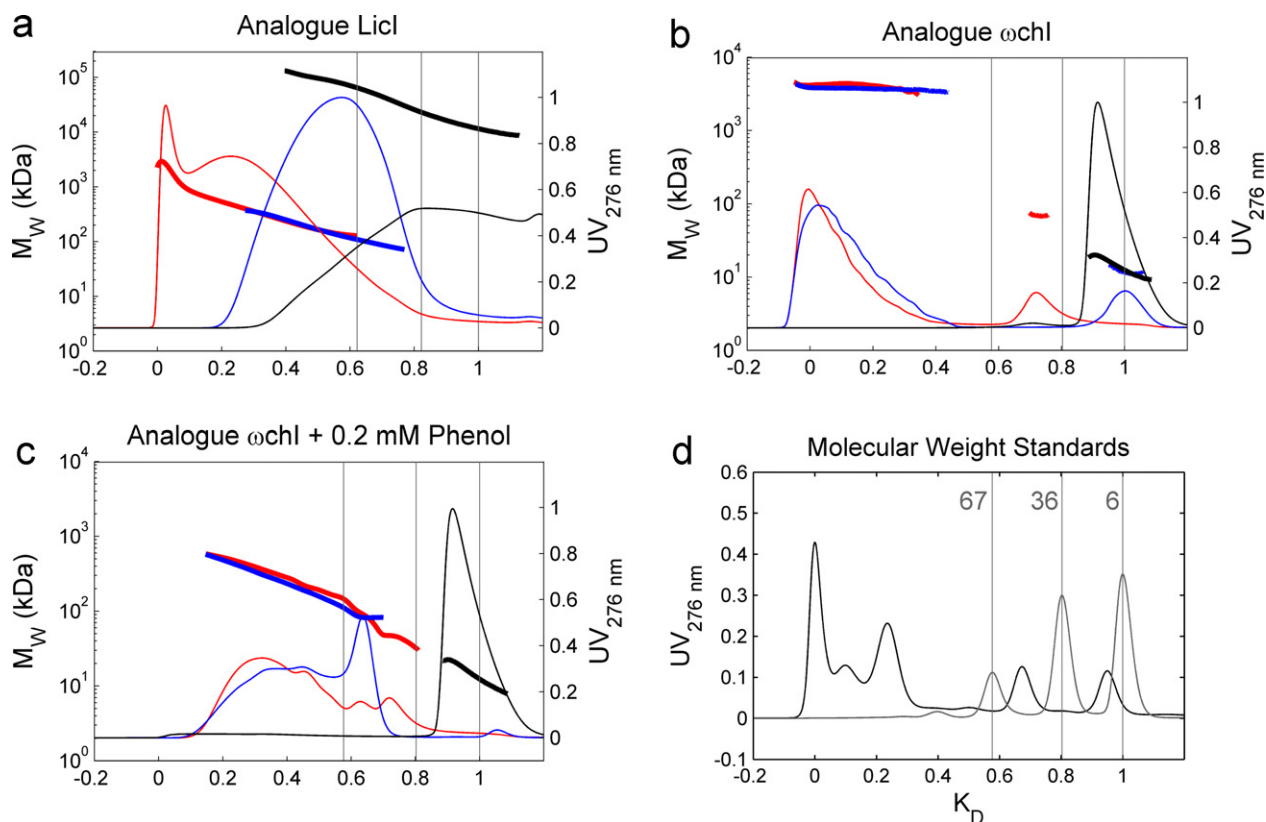
Fig. 2. SEC–MALS chromatograms of insulin analogue Lys^B29 (N^ε-lithocholyl) des(B30) human insulin (a) and Lys^B29 (N^ε ω-carboxyheptadecanoyl) des(B30) human insulin (b and c) formulated with 0 (black), 3 (blue), and 6 Zn(II)/6 Ins (red). The eluent contained 10 mM Tris–HCl, pH 7.4, 140 mM NaCl, and 0.01% NaN₃ and in (c) 0.2 mM phenol was added to the eluent. The following standards were used (d, black): blue dextran (2000 kDa), thyroglobulin (669 kDa), ferritin (440 kDa), ovalbumin (43 kDa) and, ribonuclease (12.6 kDa), and (d, grey): HSA (67 kDa), cobalt (III) insulin (hexameric, 35 kDa), and B9Asp/B27Glu insulin (monomeric, 6 kDa). The weight average molecular weight calculated with Zimm's equation is shown as a line through the chromatogram (in the same colour as the UV₂₇₆ trace).

assembly of ~3000–4600 kDa. The results obtained by Havelund et al. [25] where ωchI_3Zn eluted in the void volume of the Sephacryl S-300 GL column (>1500 kDa) are in accordance with the results presented here. In the ωchI_3Zn sample, a minor peak (K_D = 1, mass fraction of 13%) chromatographically corresponding to a monomer or a dimer was observed (monomers and dimers cannot be distinguished on this SEC column); formation of a dimer was further supported by a determined M_W of 12 kDa. The presence of dimers in ωchI_3Zn indicates that a higher Zn(II) content is needed to obtain full hexamer formation. Another minor peak was found in ωchI_6Zn with a calculated M_W of 70 kDa (K_D = 0.72; mass fraction of 13%) corresponding to a dihexamer.

The effect of the injected mass on the column was tested, which showed that in concentrations down to 150 μM ωchI_3Zn and ωchI_6Zn both eluted in the void volume (data not shown). Thus, potential concentration effects on self-association of ωchI in the presence of zinc were not visible from these investigations. With decreasing mass of ωchI_0Zn (equally down to 150 μM, data not shown), the corresponding peak moved towards lower MM (K_D = 1), indicating that the monomer/dimer equilibrium is pushed further towards the monomer state as a result of the lower protein concentration.

In all the ωchI experiments formulated with zinc the protein eluted in the void volume, i.e. outside the separation range of the column; however, it cannot be ruled out that potential differences do exist but were not resolved in our experiments. Hence, complementary studies are needed to further characterise the system. It is, however, apparent from these experiments that zinc ions do not influence the state and size of the high MM self-assemblies of the two analogues in the same way, and differences were present in the low-MM species (see Table 1 and Fig. 2a and b).

3.3. Self-association of Lys^B29 (N^ε ω-carboxyheptadecanoyl) des(B30) human insulin slowed down by addition of phenol to the eluent

The addition of low concentrations of phenol to the eluent made it possible to slow down the self-association process and obtain separation of differently sized species of analogue ωchI. Phenol concentrations of 0.1, 0.15, 0.2, 0.6, 2, and 6 mM were tested (data not shown). The different concentrations changed the degree of self-association from massive multi-hexamers eluting in the void volume of the column (0–0.15 mM) to oligomers of the size of a dihexamer (0.6–6 mM) (data not shown).

Under these elution conditions, the chromatographic profile of ωchI_0Zn was essentially the same as in the phenol-free elution buffer; an asymmetrical peak with a M_W slope of 8–23 kDa indicating oligomers smaller than a hexamer in equilibrium.

From Fig. 2c it is obvious that the addition of phenol to the elution buffer reduces the self-association for the zinc containing samples. In the presence of 0.2 mM phenol a different elution profile was achieved for ωchI_3Zn (see Fig. 2c); however, the monomer/dimer peak from the phenol-free system can still be observed (K_D of >1). The elution profile was more jagged, with emerging individual peaks, indicating the formation of individual oligomers in a more controlled manner than what was observed for licI. The ωchI_3Zn formulation eluted in a broad peak with one pronounced peak with a K_D of 0.65 (M_W ~ 82 kDa), as well as a small monomer/dimer peak. In the latter case a weak light scattering signal did not allow calculation of a reliable M_W.

In ωchI_6Zn, a more pronounced separation of the peaks is distinguishable, albeit without baseline separation. Two overlapping low-MM peaks are seen with a K_D of 0.65 and 0.72, respectively.

The M_W obtained for these two peaks (47 and 95 kDa) does not correspond to two distinct oligomeric species of insulin, such as a hexamer or a dihexamer, but they indicate the existence of two different equilibria between different oligomeric insulin species. This is supported by the sloping M_W of the smallest peak, showing a distribution from 30 to 50 kDa.

The peak in the ωchI_6Zn sample (K_D of 0.72 in Fig. 2b and c) – found both in the absence and presence of phenol in the eluent – had M_W values of 70 and 30–50 kDa, respectively. This peak was thus probably due to equilibrium between hexameric and dihexameric species of the insulin analogue in both systems. Because the tense state is thought to be the self-association prone state, it could be speculated that we here observe an equilibrium between hexamers and dihexamers in the R-state with no faces in the T-state exposed to the surroundings, which may be the reason for no further self-association.

In the presence of 0.2 mM phenol, the peak observed for both ωchI_3Zn and ωchI_6Zn (K_D of 0.65 in Fig. 2c) has M_Ws of 82 and 95 kDa, respectively. These M_Ws do not correspond with the elution between hexameric Co(III) Insulin and HSA of 67 kDa. The different M_Ws of this peak also indicate the existence of an equilibrium. The M_W suggests an equilibrium between dihexameric species and something larger. The absence of the smaller peak (proposed to be the hexamer/dihexamer equilibrium) in ωchI_3Zn could suggest that the smallest species participating in self-association is a dihexamer, and the peak therefore represents an equilibrium between dihexameric and tetra–hexameric species. Such a dihexameric species has previously been reported for IDeg, which also self-associates into multi-hexamers [21]. The oligomers of this equilibrium would then have to be in the T-state in order to facilitate self-association.

These results clearly illustrate that both analogues form vast multi-hexameric species when formulated with zinc ions in a SEC experiment mimicking s.c. injection. Furthermore, it is shown that the degree of self-association of the two analogues is different depending on the amount of zinc present in the formulation and the injected mass of the protein. And finally, low concentrations of phenol slow down the otherwise fast oligomerisation process of ωchI, such that smaller species can be identified.

3.4. Shape prediction from R_g, R_H and M_W

The MALS and DLS signal was used to achieve information about the molecular size. The relationship between R_g and R_H or R_g and M_W both give an indication about the shape of the species in solution. These parameters have been used for shape prediction of micellar and colloidal systems [42–44].

Fig. 3 shows the R_g and R_H calculated for ωchI_6Zn in the elution system containing 0.2 mM phenol. The shape factor, ρ, equal to the ratio between R_g and R_H provides an indication of the deviation from a homogenous spherical particle. That is, a ρ value of 0.78 or >2 correspond to a spherical or a rod-shaped particle, respectively. ρ was calculated at specific points through the chromatogram ($\rho_{\omega chI\_6Zn}$ = 1.7, 1.5, 1.3, and 1.3, see Fig. 3). The development of R_g and R_H and the ρ values calculated through the chromatogram clearly shows a change from a more spherical shape at low-MM going towards a more elongated rod-shaped particle at high-MM (ρ values and positions in the chromatogram can be seen in Fig. 3). According to the manufacturer, the lowest R_g measurable by the equipment is 10 nm; therefore, the ρ values calculated from an R_g below this level should be taken as an indication of the shape. ωchI_3Zn showed approximately the same trend in R_g and R_H through the chromatogram as that seen for ωchI_6Zn (data not shown).

Another method for analysing the shape of a protein is using a plot of $\log(M_W)$ versus $\log(R_g)$. The slopes (ν) of a rod, coil, and a
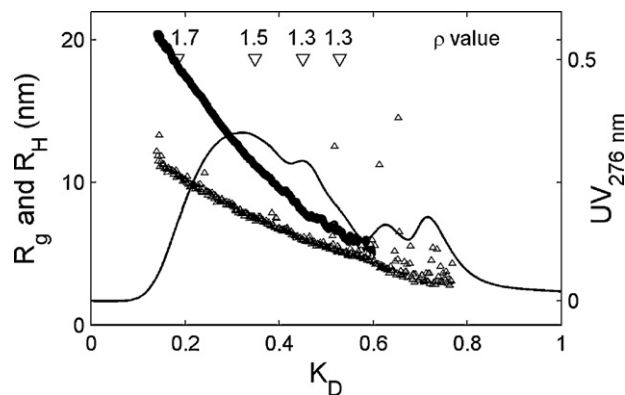
Fig. 3. Chromatograms showing R_g and R_H of the sample ωchI_6Zn (black). R_g and R_H, which were calculated from the SLS and DLS signal during chromatographic separation, are shown as triangles and circles, respectively. The shape factor, ρ (=R_g/R_H), is calculated for individual points through the chromatogram. This ratio describes how much the shape of a particle deviates from a sphere, where a sphere and a rod have a ρ-value of 0.78 and >2, respectively.
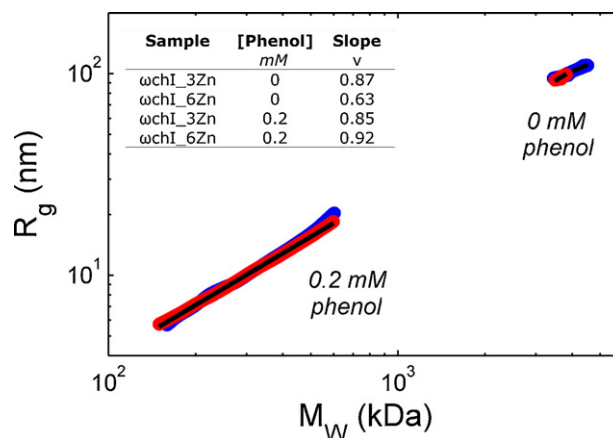
Fig. 4. A conformation plot is shown, where M_W is plotted against R_g. The slope of a fitted curve (ν) to the data can give an indication about the shape of the particle in solution. The slopes for a rod, coil, and a sphere are 1, 0.5, and 0.33, respectively. Samples ωchI_3Zn (red) and ωchI_6Zn (blue) (0 and 0.2 mM phenol in the eluent) are shown in the plot. The black lines represent fits to the data and the corresponding slopes are listed in the table for each sample.

sphere are 1, 0.5, and 0.33 [39], respectively. In Fig. 4, M_W is plotted against R_g for ωchI_3Zn and ωchI_6Zn in 0.2 mM phenol. The individual samples in each elution system are again quite similar, indicating shapes of the self-associated samples between coil and rod. For ωchI_3Zn slopes of 0.87 and 0.85 were observed in the absence and presence of phenol, respectively. For ωchI_6Zn the slopes vary more and were found to be 0.63 (without phenol) and 0.92 (with phenol).

Both methods pointed towards an elongated shape for ωchI in the presence of 3 and 6 Zn(II)/6 Ins. A similar analysis licI would be valuable, however, the R_g and R_H values were either undeterminable or outside the range of the instrument to facilitate any analysis or speculations regarding the shape of these samples.

The elongated rod-like shape furthermore explains the elution profiles of ωchI, where in a variety of concentrations and zinc content ωchI always elutes in the void volume. The exclusion of particles on a gel filtration column is highly dependent on the shape as well as the MM. Therefore, the particles elute according to their R_g, which is larger for a rod compared to a sphere of the same MM; thus a SEC column has a much smaller separation range for rod-shaped particles than for spherical particles. It is therefore not surprising

that this analogue elutes in the void volume under the conditions tested here.

4. Conclusion

The SEC–MALS based results presented in this paper shed light on the mechanism of self-association of the two structurally different insulin analogues, ωchI and licI. It is shown for both analogues that the degree of self-association is affected by the amount of zinc ions present in the pharmacological formulation.

In the case of licI, the sizes of the high MM associates are directly dependent on the zinc concentration. Furthermore, we propose that licI also aggregates in the absence of zinc. This self-association is expected to be of a very different nature, where monomers and dimers can be the building blocks of the large complexes. This information was not revealed by gel filtration alone, but by the combination of SEC and MALS. Without the M_W determined with MALS this significant difference in mass would not have been observed. These observations strongly underline the importance of using an absolute MM method, and not only rely on ideal separation conditions and standards; thus using orthogonal methods when investigating complex self-assembling macromolecular systems is important.

In contrast, self-association of ωchI formulated with zinc results in high MM self assembly. The addition of phenol in low concentrations to the SEC elution system was necessary to obtain complexes of smaller and varying sizes. In the absence of zinc, ωchI was shown to exist in equilibrium between oligomers smaller than a hexamer, underlining that further self-association of this analogue is dependent on the presence of divalent metal ion ligands. Lastly, based on the observations described here, it can be speculated that the dihexamer is the smallest building block in the self-association of ωchI.

Finally, analysis of M_W, R_g, and R_H determined by MALS suggests that the self-associated samples of ωchI formulated with zinc are rod-shaped. It was not possible to carry out the parallel analysis for licI.

The results reported here show a significant difference in self-association behavior between the two types of protracted insulin analogues. The SEC–MALS result presented here underlines the substantial complexity in high MM self-assembly of licI and ωchI. Further investigation into the processes with other techniques is necessary to broaden the knowledge of the two systems representing a new generation of soluble basal insulin analogues, with long and peak-less pharmacokinetic profiles.

References

[1] S. Wild, G. Roglic, A. Green, R. Sicree, H. King, Diabetes Care 27 (2004) 1047.
[2] T.L. Blundell, J.F. Cutfield, S.M. Cutfield, E.J. Dodson, G.G. Dodson, D.C. Hodgkin, D.A. Mercola, Diabetes 21 (1972) 492.
[3] J.F. Hansen, Biophys. Chem. 39 (1991) 107.
[4] S. Hvidt, Biophys. Chem. 39 (1991) 205.
[5] J. Brange, U. Ribel, J.F. Hansen, G. Dodson, M.T. Hansen, S. Havelund, S.G. Melberg, F. Norris, K. Norris, L. Snel, A.R. Sorensen, H.O. Voigt, Nature 333 (1988) 679.
[6] D.L. Bakaysa, J. Radziuk, H.A. Havel, M.L. Brader, S. Li, S.W. Dodd, J.M. Beals, A.H. Pekar, D.N. Brems, Protein Sci. 5 (1996) 2521.
[7] R.H. Becker, Diabetes Technol. Ther. 9 (2007) 109.
[8] J. Markussen, I. Diers, P. Hougaard, L. Langkjaer, K. Norris, L. Snel, A.R. Sorensen, E. Sorensen, H.O. Voigt, Protein Eng. 2 (1988) 157.
[9] S.G. Ashwell, P.D. Home, Expert Opin. Pharmacother. 2 (2001) 1891.
[10] P. Kurtzhals, Endocrinol. Metab. Clin. North Am. 36 (Suppl. 1) (2007) 14.
[11] W.D. Kohn, R. Micanovic, S.L. Myers, A.M. Vick, S.D. Kahl, L. Zhang, B.A. Strifler, S. Li, J. Shang, J.M. Beals, J.P. Mayer, R.D. DiMarchi, Peptides 28 (2007) 935.
[12] P. Kurtzhals, S. Havelund, I. Jonassen, B. Kiehr, U.D. Larsen, U. Ribel, J. Markussen, Biochem. J. 312 (1995) 725.
[13] J.L. Whittingham, S. Havelund, I. Jonassen, Biochemistry 36 (1997) 2826.
[14] M. Hamilton-Wessler, M. Ader, M. Dea, D. Moore, P.N. Jorgensen, J. Markussen, R.N. Bergman, Diabetologia 42 (1999) 1254.
[15] J. Markussen, S. Havelund, P. Kurtzhals, A.S. Andersen, J. Halstrom, E. Hasselager, U.D. Larsen, U. Ribel, L. Schaffer, K. Vad, I. Jonassen, Diabetologia 39 (1996) 281.
[16] K. Hermansen, S. Madsbad, H. Perrild, A. Kristensen, M. Axelsen, Diabetes Care 24 (2001) 296.
[17] P. Vague, J.L. Selam, S. Skeie, I. De Leeuw, J.W. Elte, H. Haahr, A. Kristensen, E. Draeger, K. Sakabe, N. Sakabe, N.M. Vijayan, Diabetes Care 26 (2003) 590.
[18] S. Havelund, A. Plum, U. Ribel, I. Jonassen, A. Volund, J. Markussen, P. Kurtzhals, Pharm. Res. 21 (2004) 1498.
[19] I. Jonassen, S. Havelund, U. Ribel, A. Plum, M. Loftager, T. Hoeg-Jensen, A. Volund, J. Markussen, Pharm. Res. 23 (2006) 49.
[20] B. Zinman, G. Fulcher, P.V. Rao, N. Thomas, L. Endahl, T. Johansen, A. Lewin, J. Rosenstock, M. Pinget, C. Mathieu, Diabetes 59 (2010) A11.
[21] I. Jonassen, S. Havelund, U. Ribel, T. Hoeg-Jensen, D. Bjerre Steensgaard, T. Johansen, H. Haahr, E. Nishimura, P. Kurtzhals, Diabetes 59 (2010) A11.
[22] T. Heise, C. Tack, B.M. Cuddihy, J. Davidson, D. Gouet, A. Liebl, E.R. Bobillo, H. Mersebach, P. Dykiel, R. Jorde, Diabetes 59 (2010) A11.
[23] I. Jonassen, S. Havelund, U. Ribel, T. Hoeg-Jensen, D.B. Steensgaard, T. Johansen, H. Haahr, E. Nishimura, P. Kurtzhals, Diabetologia 53 (2010).
[24] L. Schäffer, P. Balschmidt, Patent WO 97/31022 (1997).
[25] S. Havelund, P. Balschmidt, I. Jonassen, T. Hoeg-Jensen, Ch. WO 99/21888 (1999).
[26] J.L. Whittingham, I. Jonassen, S. Havelund, S.M. Roberts, E.J. Dodson, C.S. Verma, A.J. Wilkinson, G.G. Dodson, Biochemistry 43 (2004) 5987.
[27] U. Derewenda, Z. Derewenda, E.J. Dodson, G.G. Dodson, C.D. Reynolds, G.D. Smith, C. Sparks, D. Swenson, Nature 338 (1989) 594.
[28] M.L. Brader, N.C. Kaarsholm, R.W. Lee, M.F. Dunn, Biochemistry 30 (1991) 6636.
[29] G. Bentley, E. Dodson, G. Dodson, D. Hodgkin, D. Mercola, Nature 261 (1976) 166.
[30] E.N. Baker, T.L. Blundell, J.F. Cutfield, S.M. Cutfield, E.J. Dodson, G.G. Dodson, D.M. Hodgkin, R.E. Hubbard, N.W. Isaacs, C.D. Reynolds, Philos. Trans. R. Soc. Lond. B: Biol. Sci. 319 (1988) 369.
[31] N.C. Kaarsholm, H.C. Ko, M.F. Dunn, Biochemistry 28 (1989) 4427.
[32] P.S. Brzovic, W.E. Choi, D. Borchardt, N.C. Kaarsholm, M.F. Dunn, Biochemistry 33 (1994) 13057.
[33] S. Havelund, I. Jonassen, P. Balschmidt, T. Hoeg-Jensen, US Patent 6451762 B1 (2002).
[34] L. Heinemann, A.A.R. Starke, L. Heding, I. Jensen, M. Berger, Diabetologia 33 (1990) 384.
[35] P. Kurtzhals, U. Ribel, Diabetes 44 (1995) 1381.
[36] J. Wen, T. Arakawa, J.S. Philo, Anal. Biochem. 240 (1996) 155.
[37] R. Pecora, Annu. Rev. Biophys. Bioeng. 1 (1972) 257.
[38] W. Burchard, in: S.E. Harding, D.B. Sattelle, V.A. Bloomfield (Eds.), Laser Light Scattering in Biochemistry, The Royal Society of Chemistry, 1992, p. 3 (Chapter 1).
[39] J.E. Rollings, in: S.E. Harding, D.B. Sattelle, V.A. Bloomfield (Eds.), Laser Light Scattering in Biochemistry, The Royal Society of Chemistry, 1992, p. 275 (Chapter 19).
[40] G.D. Smith, E. Ciszak, L.A. Magrum, W.A. Pangborn, R.H. Blessing, Acta Crystallogr. D: Biol. Crystallogr. 56 (2000) 1541.
[41] T. de la Garcia, M.L. Huertas, B. Carrasco, Biophys. J. 78 (2000) 719.
[42] C.Y. Young, P.J. Missel, N.A. Mazer, G.B. Benedek, M.C. Carey, J. Phys. Chem. 82 (1978) 1375.
[43] T. Matsuoka, K. Yasuda, K. Yamamoto, S. Koda, H. Nomura, Colloids Surf. B: Biointerfaces 56 (2007) 72.
[44] M. Baalousha, F.V. Kammer, M. Motelica-Heino, H.S. Hilal, P. Le Coustumer, J. Chromatogr. A 1104 (2006) 272.